

# Design and Implementation of a $3 \times 3$ Orthogonal Beam-Forming Network for Pattern-Diversity Applications

Guan-Xi Zhang<sup>1, \*</sup>, Bao-Hua Sun<sup>1</sup>, Li Sun<sup>1</sup>, Jian-Ping Zhao<sup>2</sup>,  
Yang Geng<sup>2</sup>, and Rui-Na Lian<sup>1</sup>

**Abstract**—An orthogonal beam-forming network (BFN) is proposed for 4G pattern-diversity applications. Different from the traditional Butler beam-forming networks with  $2^N$  orthogonal beams, the orthogonal BFN, composed of three  $180^\circ$  hybrids and a  $90^\circ$  phase shifter, provides three orthogonal beams. Design procedure of the orthogonal BFN based on the factorization of its transmission matrix is derived. Moreover, in order to implement the proposed orthogonal BFN with low insertion loss, a rat-race has been used to realize unequal power distribution between its two output ports. The measured scattering parameters of the orthogonal BFN are compared with the analytical and the simulated scattering parameters, validating the expected behavior. In addition, by varying the output power ratio of the non-equi-amplitude  $180^\circ$  hybrid, the performance of the orthogonal BFN is improved when the proposed orthogonal BFN is used in an antenna array.

## 1. INTRODUCTION

In present wireless communication systems, increased channel capacity, improved transmission quality with minimum interference and multipath phenomena are severe design challenges. Multibeam antenna arrays have become more and more important. They can provide an increase in the system capacity, give the possibility of space division multiple access implementations [1, 2], and offer the higher signal to interference ratio, thus improving overall system performance.

One typical method to implement a multi-beam antenna is to use an antenna array fed by a beam-forming network (BFN). Since the early 1960s, different solutions such as Blass matrix [3], Nolen matrix [4], Rotman lens [5] and Butler matrix [6] have been proposed. Among these matrices, the Butler matrix has obtained particular attention in literature [6, 7] and wide applications as it is theoretically lossless and employs the minimum number of components. The Butler matrix, in its original design, only allows  $N = 2^p$  inputs and  $N = 2^p$  outputs, with  $p$  an integer. However, in modern communication systems, sometimes the number of orthogonal beams is not  $2^p$  and it is not necessary to design so many beams. An orthogonal BFN with three orthogonal beams, in general, is important for pattern-diversity applications [8].

Based on the factorization of the transmission matrix, the procedure of synthesizing the orthogonal BFN for  $N = 6, 8$  and  $9$  orthogonal beams is described in [9]. Compared with the design procedure, the implementation of the orthogonal BFN is also important and difficult which is not discussed in [9].

In this paper, the design and implementation of an orthogonal BFN with three inputs and three outputs ( $3 \times 3$ ) is presented, which can realize three orthogonal beams. The orthogonal BFN has

---

*Received 28 May 2014, Accepted 10 August 2014, Scheduled 18 August 2014*

\* Corresponding author: Guan-Xi Zhang (gxzhang\_xidian@126.com).

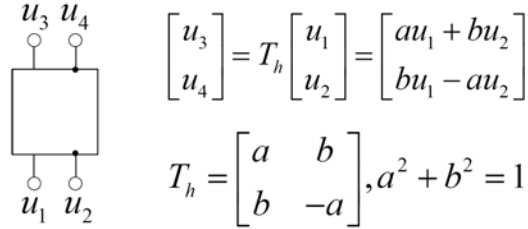
<sup>1</sup> National Laboratory of Science and Technology on Antennas and Microwaves, Xidian University, Xi'an, Shaanxi 710071, China.

<sup>2</sup> System Technology Research Department, WN [Carrier Network BG], Huawei Technologies Co., Ltd, Shanghai, China.

advantage of simple structure in which only four common components is needed. A new non-equi-amplitude rat-race is designed via even-odd mode analysis. In addition, when the proposed  $3 \times 3$  orthogonal BFN is used in an antenna array, the performance of the  $3 \times 3$  orthogonal BFN is improved by adjusting the output power ratio of the non-equi-amplitude rat-race, owing to the characteristic of the taper distribution in a linear antenna array.

## 2. SYNTHESIS FOR THE PROPOSED ORTHOGONAL BFN

As key components, three  $180^\circ$  hybrids are used in the proposed orthogonal BFN. The general schematic of a  $180^\circ$  hybrid and its orthogonal transmission matrix are shown in Fig. 1. Where  $u_1$  and  $u_2$  are input voltages and  $u_3$  and  $u_4$  are output voltages. Given  $a = b$ , the  $180^\circ$  hybrid is an equi-amplitude (3 dB) one. While given  $a \neq b$ , the  $180^\circ$  hybrid is a non-equi-amplitude one, and the output powers ratio is  $p = (a/b)^2$ .



$$\begin{bmatrix} u_3 \\ u_4 \end{bmatrix} = T_h \begin{bmatrix} u_1 \\ u_2 \end{bmatrix} = \begin{bmatrix} au_1 + bu_2 \\ bu_1 - au_2 \end{bmatrix}$$

$$T_h = \begin{bmatrix} a & b \\ b & -a \end{bmatrix}, a^2 + b^2 = 1$$

**Figure 1.**  $180^\circ$  hybrid and its transmission matrix.

In order to realize three orthogonal beams, the transmission block  $T$  of the scattering matrix represents a symmetrical unitary matrix as follows [9]:

$$T = \frac{\sqrt{3}}{3} \begin{bmatrix} 1 & 1 & 1 \\ 1 & -\frac{1}{2} - \frac{\sqrt{3}}{2}i & -\frac{1}{2} + \frac{\sqrt{3}}{2}i \\ 1 & -\frac{1}{2} + \frac{\sqrt{3}}{2}i & -\frac{1}{2} - \frac{\sqrt{3}}{2}i \end{bmatrix} \quad (1)$$

The transmission block  $T$  can be represented as a product of three factors of size  $3 \times 3$  based upon second application of Givens rotations,

$$T = YQY \quad (2)$$

where  $Y$  is a square, real, symmetric, and orthogonal matrix, and it implies a balanced  $180^\circ$  hybrid.

$$Y = \begin{bmatrix} 1 & 0 & 0 \\ 0 & \frac{\sqrt{2}}{2} & \frac{\sqrt{2}}{2} \\ 0 & \frac{\sqrt{2}}{2} & -\frac{\sqrt{2}}{2} \end{bmatrix} \quad (3)$$

Based on matrix manipulation that the inverse of the matrix  $Y$  equals itself,  $Q$  is equal to  $YTY$  as follows:

$$Q = \begin{bmatrix} \frac{\sqrt{3}}{3} & \frac{\sqrt{6}}{3} & 0 \\ \frac{\sqrt{6}}{3} & -\frac{\sqrt{3}}{3} & 0 \\ 0 & \frac{\sqrt{2}}{2} & -i \end{bmatrix} = \begin{bmatrix} Q_1 & \\ & iQ_2 \end{bmatrix} \quad (4)$$

where

$$Q_1 = \begin{bmatrix} \frac{\sqrt{3}}{3} & \frac{\sqrt{6}}{3} \\ \frac{\sqrt{6}}{3} & -\frac{\sqrt{3}}{3} \end{bmatrix}; \quad Q_2 = [-1] \quad (5)$$

Here  $Q_1$  and  $Q_2$  imply a non-equi-amplitude  $180^\circ$  hybrid of which the outputs power ratio is 2 : 1 and a  $90^\circ$  phase shifter, respectively.

Therefore, the full schematic of the  $3 \times 3$  orthogonal BFN can be realized by using a  $90^\circ$  phase shifter, a non-equi-amplitude and two equi-amplitude  $180^\circ$  hybrids shown in Fig. 2.

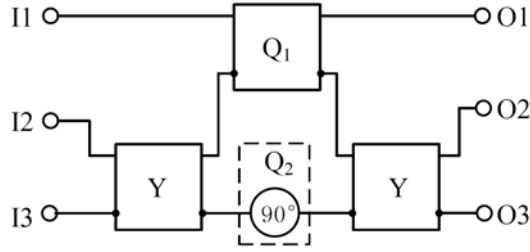


Figure 2. Full schematic of the proposed orthogonal BFN.

### 3. IMPLEMENTATION OF THE PROPOSED ORTHOGONAL BFN

In order to realize the  $3 \times 3$  orthogonal BFN, a microstrip implementation with low loss is presented. The FEM-based Ansoft HFSS 14.0 simulator is used to simulate and optimize the  $180^\circ$  hybrid and the  $3 \times 3$  orthogonal BFN. The substrate in the simulation is a dielectrically homogeneous material of dielectric constant  $\epsilon_r = 2.65$ , thickness  $h = 1$  mm and loss tangent  $\tan \delta = 0.002$ .

The design of the equi-amplitude hybrid  $Y$  and the non-equi-amplitude hybrid  $Q_1$  is presented and then connected according to the design presented in Fig. 2. The absolute phase shifters of the  $180^\circ$  hybrid have also been considered. The design and the performance of each component of the proposed orthogonal BFN are described in details in the following subsections.

#### 3.1. Equi-Amplitude and Non-Equi-Amplitude Rat-Races

The equi-amplitude  $180^\circ$  hybrid  $Y$  is achieved by the rat-race shown in Fig. 3 where  $Z_1$  and  $Z_2$  are the characteristic impedances of the transmission lines [10]. Based on the normal rat-race, a  $180^\circ$  hybrid  $Q_1$  has been designed with 3 dB amplitude difference and  $0^\circ/180^\circ$  phase difference between the two output ports. Using the even-odd mode analysis, it is known that the input impedance  $Z_0$  of the ports of the rat-race and the output power ratio  $p$  can be expressed by  $Z_1$  and  $Z_2$  as follows:

$$Z_0 = \frac{Z_1 Z_2}{\sqrt{Z_1^2 + Z_2^2}} \quad (6)$$

$$p = (Z_1/Z_2)^2 \quad (7)$$

The equi-amplitude rat-race  $Y$  and the non-equi-amplitude rat-race  $Q_1$  of which the output power ratio is  $2 : 1$  are realized over the frequency range of 2.3–2.7 GHz. According to Equations (6) and (7), the values of  $Z_1$  and  $Z_2$  in the two rat-races are obtained and listed in Table 1. The characteristic impedances of the input microstrip line  $Z_0$  is equal to  $50 \Omega$ . Using the characteristic impedance equations of the microstrip transmission line [8], the transmission line parameters of  $Z_1$  and  $Z_2$  are calculated and listed

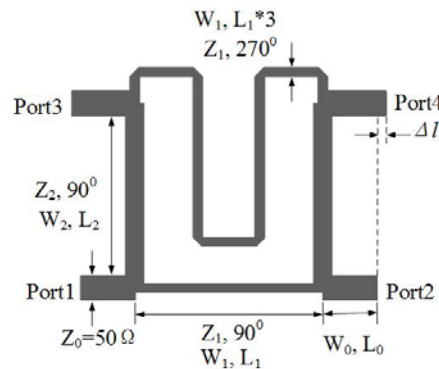


Figure 3. Configuration of the designed rat-race.

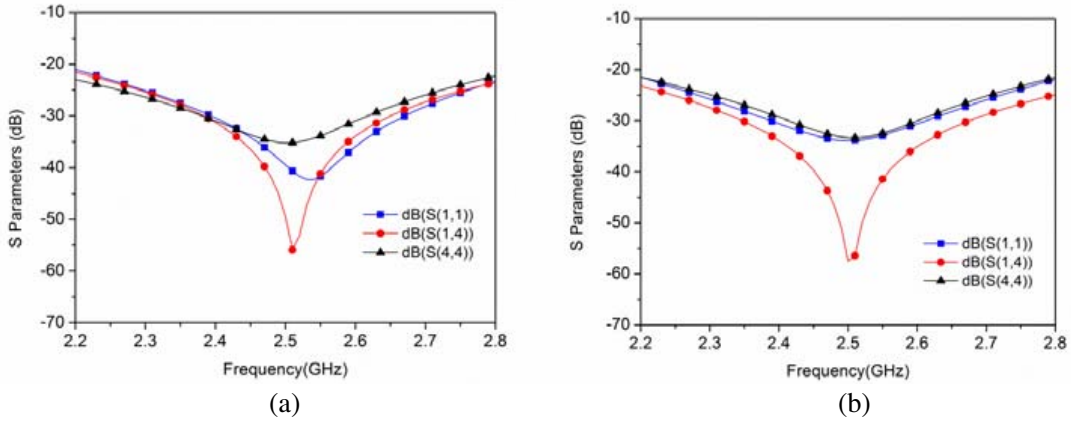
**Table 1.** Calculated parameters of two rat-races. (Length-unit: mm).

Rat-race	$Z_1$ ( $\Omega$ )		$Z_2$ ( $\Omega$ )		$Z_0$ ( $\Omega$ )		
	$W_1$	$L_1$	$W_2$	$L_2$	$W_0$	$L_0$	$\Delta l$
Y	70.7		70.7		50.0		
	1.5	20.6	1.5	17.9	2.7	6.0	1.0
$Q_1$	86.6		61.2		50.0		
	1.0	20.9	2.0	17.8	2.7	6.0	1.0

in Table 1. The length difference  $\Delta l$  between the two microstrips is used to adjust the phase difference to improve the performance of the  $S$  parameters in all ports simultaneously. All the optimized geometry parameters ( $W_1, W_2, L_1, L_2, \Delta l$ ) of the equi-amplitude and non-equi-amplitude rat-races are listed in Table 1.

As shown in Figs. 4(a) and (b), the return losses and isolations of the two rat-races are better than 25 dB over the frequency range of 2.3–2.7 GHz. Compared with the desired values, the simulated maximum amplitude discrepancy is within  $\pm 0.3$  dB and the maximum phase discrepancy is within  $\pm 7^\circ$  over the frequency range of 2.3–2.7 GHz as shown in Figs. 5(a) and (b).

Owing to a traditional  $270^\circ$  microstrip line in the hybrids, the bandwidth of the hybrids should be narrow. A modified form of conventional rat-race hybrid can offer a much larger bandwidth. The modified version is obtained by replacing the traditional  $270^\circ$  microstrip line of the conventional rat-race by a pair of  $90^\circ$  coupled microstrip line [11].

**Figure 4.** Simulated return losses and isolations of the rat-races. (a) The equi-amplitude rat-race Y. (b) The non-equi-amplitude rat-race  $Q_1$ .

### 3.2. The Proposed $3 \times 3$ Orthogonal BFN

The  $3 \times 3$  orthogonal BFN illustrated in Fig. 6 is proposed by combining the above designed components. It is noted that there are not any crossovers within the orthogonal BFN.  $Q_2$  is a  $90^\circ$  phase shifter which is achieved by using a simple microstrip line. To compensate the absolute phase difference caused by rat-races Y and  $Q_1$ , additional microstrip lines are added between the rat-race Y and the  $90^\circ$  phase shifter  $Q_2$ .

The measured return losses and isolations for the three input ports I1, I2, and I3 are larger than 25 dB and 30 dB at the frequency of 2.5 GHz, respectively, which are shown in Table 2. Analytical, simulated and measured transmission magnitude and phase parameters at 2.5 GHz are shown in Table 3. The simulated amplitude imbalance equals  $\pm 0.3$  dB and the maximum phase discrepancy is less than  $\pm 2^\circ$  at 2.5 GHz.

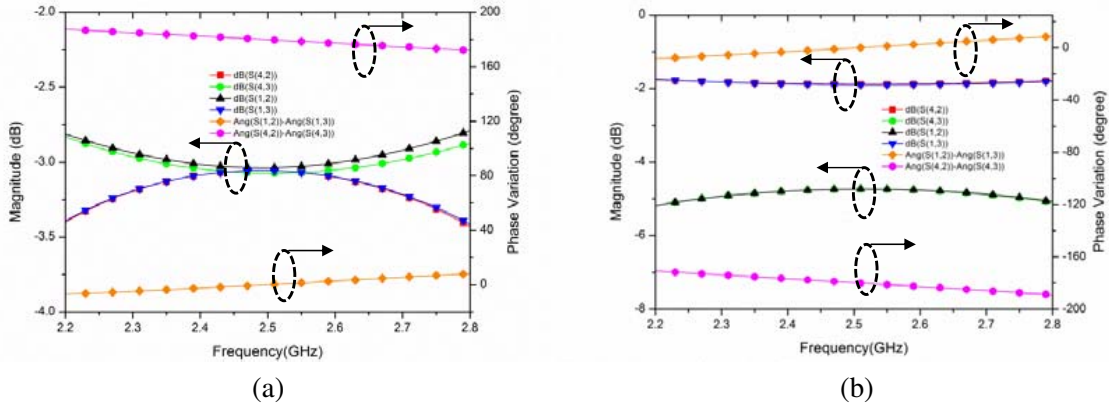


**Figure 5.** Simulated transmission characteristics of the rat-races. (a) The equi-amplitude rat-race  $Y$ . (b) The non-equi-amplitude rat-race  $Q_1$ .

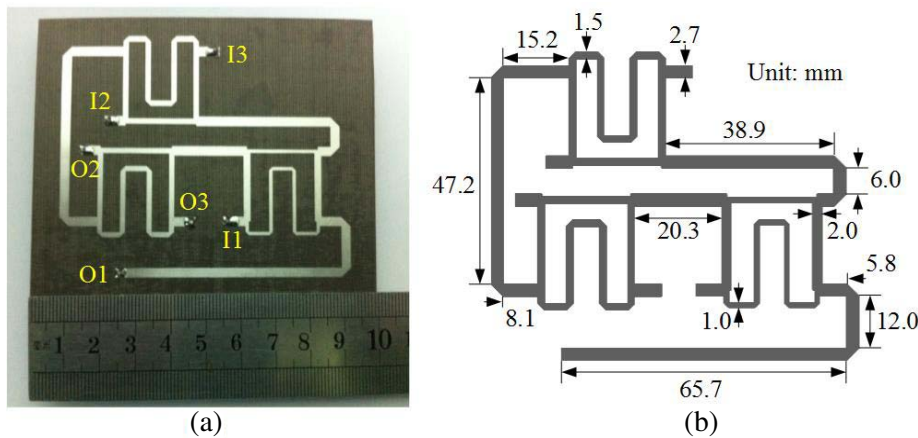


**Figure 6.** The proposed microstrip BFN. (a) Photograph. (b) Configuration.

**Table 2.** Simulated and measured isolations and return losses of the input ports I1, I2 and I3 of the proposed BFN.

$ S $ (dB)	$S(I1,I1)$	$S(I2,I2)$	$S(I3,I3)$	$S(I1,I2)$	$S(I1,I3)$	$S(I2,I3)$
Simulated	-43.8	-37.9	-46.7	-40.3	-40.0	-29.4
Measured	-35.6	-32.8	-37.4	-30.9	-29.7	-25.8

#### 4. IMPROVEMENT IN PERFORMANCE OF THE ORTHOGONAL BFN

Given that the output power ratio of rat-race  $Q_1$  increases, the amplitudes of outputs O2 and O3 of the proposed orthogonal BFN fed by I1 and I2 decrease, and the amplitude of output O1 increases. In the proposed orthogonal BFN, O1, O2 and O3 can be exchanged at random owing to that the output differential phases fed by three inputs are  $0^\circ$ ,  $120^\circ$  and  $-120^\circ$ , respectively. The amplitudes of the outputs can be presented in taper distribution by exchanging O1 and O2. The performance of the orthogonal BFN is designed when the proposed orthogonal BFN is used in an antenna array.

Given that the output power ratios of the non-equi-amplitude rat-race are  $2 : 1$  and  $4 : 1$ , the amplitude and phase difference of the outputs are listed in Tables 4(a) and (b), respectively. In order to comprise the performance the two BFNs, a linear array of three microstrip antennas in [12] at the frequency of 2.5 GHz with the array distance  $d = \lambda/2$  is used. The array fed by the two BFNs can

**Table 3.** Analytical, measured and simulated amplitude and differential phase characteristics of the proposed orthogonal BFN fed by port I1, I2 and I3. (a) Analytical values, (b) simulated values, (c) measured values.

Analytical	Amplitude (dB)			Phase differential (degree)		
	Fed by	I1	I2	I3	I1	I2
O1	-4.77	-4.77	-4.77	0	0	0
O2	-4.77	-4.77	-4.77	0	-120	-240
O3	-4.77	-4.77	-4.77	0	-240	-120

(a)

Simulated	Amplitude (dB)			Phase differential (degree)		
	Fed by	I1	I2	I3	I1	I2
O1	-4.96	-4.81	-5.00	0	0	0
O2	-4.72	-4.95	-5.07	-1.7	-123.1	-242.3
O3	-4.96	-5.02	-4.86	-0.4	-241.3	-121.5

(b)

Measured	Amplitude (dB)			Phase differential (degree)		
	Fed by	I1	I2	I3	I1	I2
O1	-5.09	-4.93	-5.13	0	0	0
O2	-4.87	-5.07	-5.15	-2.6	-122.5	-241.1
O3	-5.08	-5.09	-4.97	1.1	-242.6	-122.6

(c)

realize the normalized far field patterns shown in Fig. 7. The side-lobe levels of the beam 2 and beam 3 fed by the modified BFN have obvious suppression compared with the beams fed by the original BFN, while the main lobes of beam 2 and beam 3 are almost unchanged.

The main beam direction of the beam 1 is located at the null of the beam 2 and beam 3. The null of the beam 1 is located at the main beam directions of the beam 2 and beam 3. It is proved that the proposed BFN is orthogonal. The proposed BFN is used when the array needs to transmit (or receive)

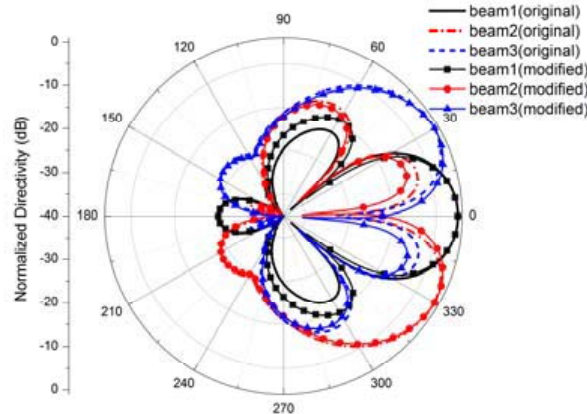


**Figure 7.** The beams of the antenna array of three microstrip antennas fed by the original and modified BFNs, respectively.

**Table 4.** The amplitude and phase difference of the outputs of the original and modified BFNs. (amplitude unit: none, phase unit: degree).

Original BFN	I1		I2		I3	
	amplitude	phase	amplitude	phase	amplitude	phase
O1	0.577	120	0.577	0	0.577	-120
O2	0.577	0	0.577	0	0.577	0
O3	0.577	-120	0.577	0	0.577	120

(a)

Modified BFN	I1		I2		I3	
	amplitude	phase	amplitude	phase	amplitude	phase
O1	0.548	114.1	0.632	0	0.548	-114.1
O2	0.632	0	0.448	0	0.632	0
O3	0.548	-114.1	0.632	0	0.548	114.1

(b)

multiple beams simultaneously in prefixed directions. Each beam is associated with an input signal at the input port, thus enhancing system performance by mitigating multipath fading and increasing channel capacity.

## 5. CONCLUSION

In this paper, a  $3 \times 3$  orthogonal BFN for pattern-diversity applications is designed and realized. In order to achieve the orthogonal BFN, a phase shifter and three  $180^\circ$  hybrids have been used. The proposed orthogonal BFN has been experimentally tested and the obtained measurement results are in very good agreement with the analytical and measured ones in terms of amplitude and phase imbalance within the operational frequency range. The authors will focus on broadband and miniaturized orthogonal BFNs by referring to [13, 14]. In addition, by varying the output power ratio of the non-equi-amplitude hybrid, the performance of the orthogonal BFN is improved when the proposed orthogonal BFN is used in an antenna array.

## REFERENCES

1. Nima, J., A. Derneryd, and Y. Rahmat-Samii, "Spatial diversity performance of multiport antennas in the presence of a Butler network," *IEEE Trans. Antennas Propagat.*, Vol. 61, No. 11, 5697–5705, Nov. 2013.
2. Xu, H.-X., G.-M. Wang, and M.-Q. Qi, "A miniaturized triple-band metamaterial antenna with radiation pattern selectivity and polarization diversity," *Progress In Electromagnetics Research*, Vol. 137, 275–292, 2013.
3. Blass, J., "Multi-directional antenna: New approach top stacked beams," *IRE Int. Convention Record*, 48–50, Pt 1, 1960.
4. Nolen, J., "Synthesis of multiple beam networks for arbitrary illuminations," Ph.D. Dissertation, Bendix Corporation, Radio Division, Baltimore, MD, Apr. 1965.
5. Rotman, W. and R. Tuner, "Wide-angle microwave lens for line source applications," *IEEE Trans. Antennas Propagat.*, Vol. 11, 623–632, 1963.
6. Butler, J. and R. Lowe, "Beam-forming matrix simplifies design of electrically scanned antennas," *IEEE Trans. Electron. Devices*, 170–173, 1961.

7. Xu, H.-X., G.-M. Wang, and X. Wang, "Compact Butler matrix using composite right/left handed transmission line," *Electron. Lett.*, Vol. 47, No. 19, 1081–1082, Sep. 2011.
8. Vassilakis, B. and S. Foo, "Dual beam sector antenna array with low loss beam forming network," U. S. Patent 8 237 619 B2, Aug. 7, 2012.
9. Sodin, L. G., "Method of synthesizing a beam-forming device for the  $N$ -beam and  $N$ -element array antenna, for any  $N$ ," *IEEE Trans. Antennas Propagat.*, Vol. 60, No. 4, 1771–1776, Apr. 2012.
10. Pozar, D. M., *Microwave Engineering*, 4th edition, 362–367, Wiley, New York, 2012.
11. Bahl, I. and P. Bhartia, *Microwave Solid State Circuit Design*, 2nd Edition, 195196, Wiley, New Jersey, 2003.
12. Balanis, C. A., *Antenna Theory Analysis and Design*, 3rd Edition, 811–814, Wiley, New Jersey, 2005.
13. Xu, H.-X., G.-M. Wang, X.-K. Zhang, and X.-L. Yang, "Novel compact dual-band rat-race coupler combining fractal geometry and CRLH TLs," *Wireless Personal Communications*, Vol. 66, No. 4, 855–864, 2012.
14. Xu, H.-X., G.-M. Wang, X. Chen, and T.-P. Li, "Broadband balun using fully artificial fractal-shaped composite right/left handed transmission line," *IEEE Microw. Wireless Compon. Lett.*, Vol. 22, No. 1, 16–18, 2012.